

DESIGNER COSMOLOGY

BRUCE A. BASSETT,^{1,2} DAVID PARKINSON,² AND ROBERT C. NICHOL²*Received 2005 March 14; accepted 2005 May 5; published 2005 May 20*

ABSTRACT

The IPSO framework allows us to optimally design experiments and surveys. We discuss the utility of IPSO with a simplified 10-parameter MCMC D -optimization of a dark energy survey. The resulting optimal number of redshift bins is typically two or three, all situated at $z < 2$. By exploiting optimization we show how the statistical power of the survey is significantly enhanced. Experiment design is aided by the richness of the figure of merit landscape that shows strong degeneracies, which means one can impose secondary optimization criteria at little cost. For example, one may choose either to maximally test a single model (e.g., Λ CDM) or to get the best model-independent constraints possible (e.g., on a whole space of dark energy models). Such bifurcations point to a future where cosmological experiments become increasingly specialized and optimization increasingly important.

Subject headings: cosmological parameters — large-scale structure of universe — surveys

Online material: color figures

1. INTRODUCTION

We have reached an enviable resonance in which improvements in detector performance and cost are allowing not only rapid gains in our fundamental knowledge of the cosmos but also the opportunity for smaller experiments to make critical contributions to that knowledge. This has resulted in a surge of interest in next-generation experiment design with over 20 major surveys in planning or construction in observational cosmology alone. Experimental cosmology has changed in a few short years into a crowded and jostling marketplace.

There are several big prizes currently at stake: *the detection of dark energy dynamics, B-mode polarization, and cosmological non-Gaussianity*. Competition, limited funding, low signal-to-noise ratio, and extreme competition mean that new surveys will need to be increasingly optimized to get the most out of them. The aims of this Letter are to show how this can be achieved in a cross-disciplinary way and to illustrate some of the rich aspects of cosmological optimization.

2. IPSO

Integrated Parameter Space Optimization (IPSO; Bassett 2004, hereafter B04) proceeds by first constructing a class of candidate survey/experiment geometries, S , labeled by survey parameters, s_i , such as areal and redshift coverage.

Second, a target parameter space, Θ , is defined, consisting of the parameters that we wish to optimally constrain (labeled θ_μ, ν, \dots). There are also typically nuisance parameters that we need to marginalize over (labeled $\varphi_{a,b,\dots}$).

Third, a figure of merit (FoM) is defined that assigns a single real number to each candidate survey. The candidate with the extremal FoM is the optimal experiment/survey. The FoM that we consider is defined by (B04)

$$\text{FoM}(s_i) = \int_{\Theta} I(s_i, \theta) p(\theta) d\theta. \quad (1)$$

Here $I(s_i, \theta)$ is a scalar that depends on the survey geometry (through the s_i) and position in Θ , and $p(\theta)$ is a “window function” that weights the different regions of the parameter space. By integrating over the parameter space, we do not make assumptions about the underlying model, which is particularly important when we have very limited knowledge of the underlying physics, as is the case with dark energy.

Most choices for $I(s_i, \theta)$ typically invoke either the parameter covariance matrix or F , the Fisher matrix, defined by

$$F_{AB} = - \left\langle \frac{\partial^2 \ln \mathcal{L}}{\partial \theta_A \partial \theta_B} \right\rangle = \sum_i \left(\frac{\partial X}{\partial \theta_A} \frac{\partial X}{\partial \theta_B} \right) \epsilon_i^{-2}(s). \quad (2)$$

Here we use $A = \{\mu, \nu, \dots; a, b, \dots\}$ to label both fundamental and nuisance parameters, \mathcal{L} is the likelihood, and $X = C_\ell, d_L, H$ represents the quantity being measured, with i labeling the redshift bin or Fourier mode as appropriate (Tegmark et al. 1998). The ϵ_i^2 are the error variances on X and depend explicitly on the survey parameters, s_i , unlike the derivatives, $\partial X / \partial \theta_A$. In computing integrals such as equation (1), this allows for significant CPU gains since the derivatives need only to be computed once.

Via the Cramér-Rao bound, F^{-1} provides the best possible covariance matrix and hence a lower bound on the achievable parameter variances. Although there are many choices for $I(s_i, \theta_\mu)$ (B04), we focus on only one for simplicity: D -optimality, defined by

$$I(s, \theta_\mu) = \log \det (F + P), \quad (3)$$

where “det” denotes matrix determinant and P is the prior precision matrix, viz., the Fisher matrix of all the relevant prior data.

Equation (3) is the gain in Shannon information or entropy over the prior. Maximizing equation (3) provides the best possible gain in constraints on the parameters θ_μ over what was available from just the prior data, P . It is known as D -optimality in the design literature. If $P = 0$, maximizing equation (3) is equivalent to minimizing the volume of the error ellipses, an alternative FoM (Huterer & Turner 2001; Frieman et al. 2003; B04). Via the general equivalence theorem, D -optimal solutions are also optimal under other figures of merit. For these reasons

¹ Department of Physics, Kyoto University, Kitashirakawa, Sakyo 606-8502 Kyoto, Japan.

² Institute of Cosmology and Gravitation, University of Portsmouth, Portsmouth PO1 2EG, UK.

it seems appropriate for cosmological applications, although, as we will see, secondary optimization criteria can be imposed at almost no cost to the primary FoM.

The nuisance parameters, such as Ω_k , Ω_m , etc., that we do not want to optimize with respect to their values, which we do not know precisely, can be easily dealt with by inverting the full Fisher matrix F_{AB} , extracting the relevant submatrix corresponding to the θ_μ , reinverting (e.g., Seo & Eisenstein 2003; B04), and then applying equation (3). Furthermore, any reasonable FoM can also be generalized to allow for the inclusion of competing surveys by simply replacing $F \rightarrow F + \mathcal{F}$, where \mathcal{F} is the sum of the Fisher matrices expected for the competing surveys. In this way IPSO will find the optimal niche with respect to the other surveys (B04).

3. OPTIMIZING CMB AND WEAK LENSING SURVEYS

When is optimization worth doing? To illustrate this, let us contrast weak lensing (wl) convergence and cosmic microwave background (CMB) surveys on the celestial sphere. In both of these cases, the Fisher matrix is a sum over ℓ (Hu & Tegmark 1999; Knox & Song 2002; Kesden et al. 2002):

$$F_{\mu\nu} = \sum_{\ell > f_{\text{sky}}^{-1/2}} \frac{2\ell + 1}{2} (N_\ell^X)^{-2} \frac{\partial C_\ell^X}{\partial \theta_\mu} \frac{\partial C_\ell^X}{\partial \theta_\nu}, \quad (4)$$

where $X = \text{CMB, wl}$, N_ℓ^X is the total noise for the survey, and f_{sky} is the fraction of the sky observed. For the CMB, we consider only one spectrum (e.g., the B -mode power spectrum). In both cases, we assume that the surveys are constrained to last a given length of time, T , and ask what is the optimal sky coverage, f_{sky} , given this constraint? For CMB experiments, we have (Knox 1995)

$$N_\ell^{\text{CMB}} \propto f_{\text{sky}}^{-1/2} \left(C_\ell^{\text{CMB}} + \frac{a f_{\text{sky}}}{T} e^{\ell^2 \sigma_b} \right), \quad (5)$$

where $T = t_{\text{pix}} N_{\text{pix}}$ is the length of the survey, a is a proportionality constant, and the N_{pix} pixels are each observed for time t_{pix} using a Gaussian beam with FWHM $\propto \sigma_b$. The first (second) term in equation (5) is the noise from sample variance (instrument noise).

CMB experiments will benefit from optimization since the competition between the terms in equation (5) creates a local minimum in the noise (Jaffe et al. 2000). To apply IPSO to the CMB, one must first choose Θ . For example, for optimal detection of deviations from the inflationary consistency conditions, the key variable is $\theta \equiv n_t + r/4.8$, where n_t is the tensor spectral index and r is the ratio of tensor to scalar quadrupole in the CMB. Single-field inflation predicts this should vanish. Hence, a high- σ detection of $\theta \neq 0$ would put severe pressure on simple inflationary models. In contrast, an experiment designed to detect B -mode polarization alone would optimize to detect r only and would lead to a different optimal area.

In contrast, for weak lensing (Kaiser 1992)

$$N_\ell^{\text{wl}} \approx f_{\text{sky}}^{-1/2} C_\ell^{\text{wl}} + \frac{\sigma_g^2}{2\sqrt{T}\bar{n}}, \quad (6)$$

where $\sigma_g^2 \sim 0.35$ is the approximately constant intrinsic ellipticity error, and the surface density of detected galaxies scales roughly as $\bar{n}\sqrt{t}$, where t is the integration time per field of view. The noise terms N_ℓ^X differ crucially when it comes to optimi-

zation of the areal coverage, f_{sky} . Unlike the CMB noise, N_ℓ^{wl} has no local minimum; the weak lensing Fisher matrix is a monotonic function of f_{sky} . Optimizing any of the FoMs simply proceeds by using the largest feasible area to minimize the sample variance.

If, in addition, the intrinsic ellipticity noise dominates the noise (as it does for the proposed *SuperNova/Acceleration Probe Wide Area Survey*), then the FoM becomes essentially independent of f_{sky} , and the gain of going to the largest area is minimal, as found by Rhodes et al. (2004).

4. OPTIMAL MEASUREMENTS OF THE HUBBLE CONSTANT

To illustrate some of the issues that one faces in applying IPSO to realistic surveys, consider the optimization of a redshift survey designed to measure the Hubble constant through observation of the radial baryon oscillations (Seo & Eisenstein 2003; Blake & Glazebrook 2003; Linder 2003a, 2003b; Amendola et al. 2004; Yamamoto et al. 2005). For clarity we assume no nuisance parameters, a flat Friedman-Lemaître-Robertson-Walker model with $\Omega_m = 0.3$, H_0 known exactly, and we ignore the constraints from d_A that a full optimization would include.

We consider a model of dark energy based on Taylor expansion in powers of $(1 - a) = z/(1 + z)$ (Chevallier et al. 2001; Linder 2003a, 2003b; Bassett et al. 2004), with $w = \rho_{\text{DE}}/\rho_{\text{DE}}$:

$$w(z) = w_0 + w_1 \frac{z}{1+z} + w_2 \frac{z^2}{(1+z)^2},$$

$$\rho_{\text{DE}} \propto (1+z)^{3(1+w_0+w_1+w_2)} \times \exp \left\{ \frac{-3z[2w_1(1+z) + w_2(2+3z)]}{2(1+z)^2} \right\}, \quad (7)$$

where $\rho_{\text{DE}}(z)$ is the dark energy density.

Comparing with equation (2), $X = E \equiv H/H_0$. Rather than the optimal area, f_{sky} , we want to know the optimal number of redshift bins, N , what redshifts they should be centered on, z_i , and how long we should observe in each bin, t_i . Again, we assume a fixed total survey time (T), so we need to optimize given the constraint $\sum_i^N t_i = T$.

We assume that the error bars scale as $\epsilon_i^{-2} = e_i t_i^\gamma$, where $e_i \propto (1+z_i)^{-\beta}$ gives the efficiency with which galaxies are detected and γ, β parameterize our ignorance. These could be treated as nuisance parameters to be marginalized over, but we find that our main results are insensitive to both over the range $\beta = 1-2$, $\gamma = 1-2$ we consider. Note that $\gamma = 1$ implies that the FoM is maximized on the boundary of the allowed redshift region (just as was the case with the weak lensing survey earlier). We focus on the case $\gamma = 2$ here for illustrative purposes. The real constraint will be significantly more complex, and we leave this issue to future work.

We restrict the bin redshifts to be in the range $0.5 < z_i < 4.5$, which is feasible for future baryon oscillation surveys such as the Kilo-Aperture Optical Spectrograph (KAOS), and set $w_2 = 0$ for clarity. We performed a Monte Carlo Markov Chain (MCMC; Christensen & Meyer 2000) optimization with the D -optimal FoM (eq. [3]) with 10 free survey parameters: $\{t_i, z_i\}$ giving the integration time and redshifts of the five bins. The effective number of bins varies dynamically because the MCMC could (and typically did) assign negligible amounts of observing time to some of the bins.

We ran multiple chains (up to 5000) with random starting

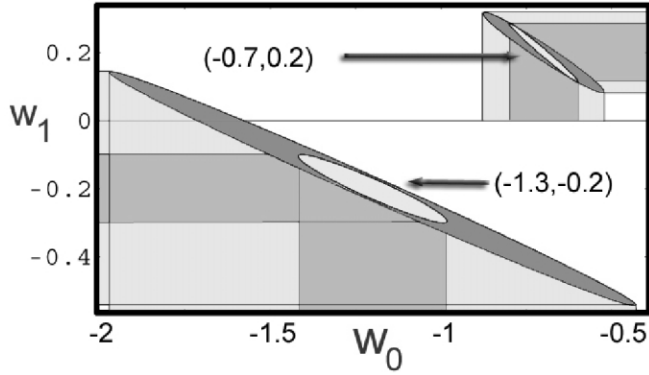


FIG. 1.—Typical D -optimality improvements on error ellipses at the two base points $(w_0, w_1) = (-1.3, -0.2)$ and $(-0.7, 0.2)$. The unoptimized survey (*outer dark ellipses*) has errors between 1.5 and 3 times larger in both w_0 and w_1 than the D -optimal survey (*inner light ellipse*) that was optimized around Λ CDM. Note the particularly significant gains in the phantom region $w_0 < -1$. [See the electronic edition of the Journal for a color version of this figure.]

configurations for the survey and used a standard Hastings-Metropolis algorithm for jump acceptance. Instead of directly performing the integral in equation (1), we used the definition $\text{FoM}(s) = (1/N) \sum_{i=1}^N I(s, \theta_a)$, where the θ_a are drawn randomly from a probability distribution based on $p(\theta_i)$ in equation (1). We chose p to be a bivariate Gaussian centered on the Λ CDM point $w_0 = -1$, $w_1 = 0$, so our optimization was chosen to detect slowly varying dark energy dynamics close to a cosmological constant.

The Fisher matrix derivatives based on equation (7) are simple to compute; e.g.,

$$\begin{aligned} \frac{\partial \rho_{\text{DE}}}{\partial w_0} &= 3\rho_{\text{DE}} \ln(1+z), \\ \frac{\partial \rho_{\text{DE}}}{\partial w_1} &= 3\rho_{\text{DE}} \left[\ln(1+z) - \frac{z}{1+z} \right]. \end{aligned} \quad (8)$$

Our unoptimized fiducial survey had five redshift bins located at $z_i = 0.6, 0.8, 1, 1.2,$ and 3 , as in Seo & Eisenstein (2003) and Amendola et al. (2004), with an equal integration time ($T/5$) assigned to each bin.

Figure 1 shows typical gains over the unoptimized survey for a near-optimal survey chosen randomly from the 5000 MCMCs, while Figure 2 shows the area of the error ellipse versus the corresponding error on w_0 for each of the 5000 locally optimal solutions. It is very clear that at an almost identical area (and FoM), there is a very wide range of error ellipse ellipticity (controlled by σ_{w_0}). In other words, there are many local maxima that come very close to matching the global maximum.

The implications of this FoM “degeneracy” for ruling out dark energy models are clarified in Figure 3, where we show the thinnest error ellipse (the diagonal “strip”), the unoptimized error ellipse, and the error ellipse with the maximal FoM, all computed at the Λ CDM point (the thinnest ellipse is shifted down for clarity).

This degeneracy offers us the chance for secondary optimization (the primary one in this case being based on the D -optimal FoM). For example, one could choose geometries that deliver the best constraints on a particular linear combination of the parameters θ_μ adapted to the degeneracy structure of the observations while sacrificing the orthogonal direction(s). This

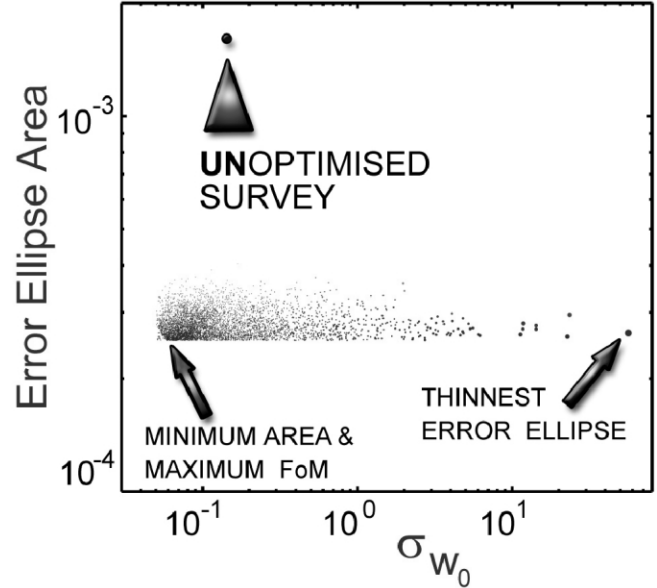


FIG. 2.—Error on w_0 (σ_{w_0}) vs. area of the error ellipse. Note the wide range of σ_{w_0} at an almost constant minimum area; σ_{w_0} effectively measures the ellipticity of the error ellipse. At a nearly constant FoM, one can optimize to obtain circular or very thin ellipses, depending on one’s aims. The size of the points is proportional to the error in w_1 . [See the electronic edition of the Journal for a color version of this figure.]

amounts to minimizing the smallest eigenvalue of the covariance matrix that may be preferable for testing dark energy dynamics in the short term.

The redshifts, z_i , and integration times, t_i , for each bin of some optimal and near-optimal surveys are shown in Figure 4 along with corresponding error bars on the Hubble rate, $H(z)$. Typically the locally optimal geometries in our 5000 chains had only two (51% of all chains) or three redshift bins (39% of all chains) with more than 5% of the total survey time. Optimal geometries with either one or five bins were extremely rare, forming less than 1% of all the locally optimal geometries (although single-bin geometries deliver the thinnest error ellipses). The preference for only a few bins arises because the dark energy models that we consider vary rather slowly with redshift; hence, it is statistically preferable to constrain w rather than dw/dz . This conclusion may change somewhat if one al-

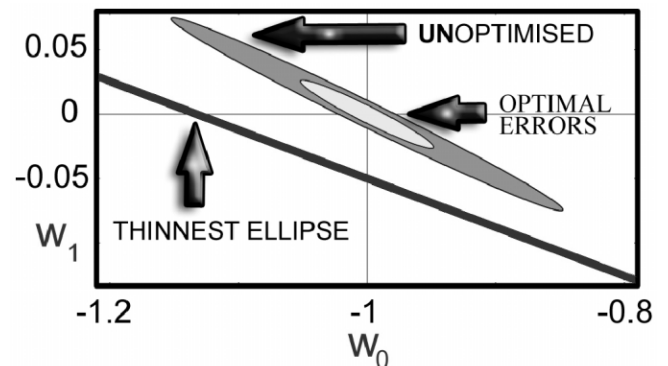


FIG. 3.—Choices in optimization. At a constant FoM, one can optimize to achieve thin error ellipses with tiny transverse errors (*diagonal dark “strip”*) or to achieve the best joint constraints on all parameters (*light ellipse*). All ellipses are computed at $w_0 = -1$, $w_1 = 0$ and reduce the total unoptimized ellipse area (*dark ellipse*) by about 600%. [See the electronic edition of the Journal for a color version of this figure.]

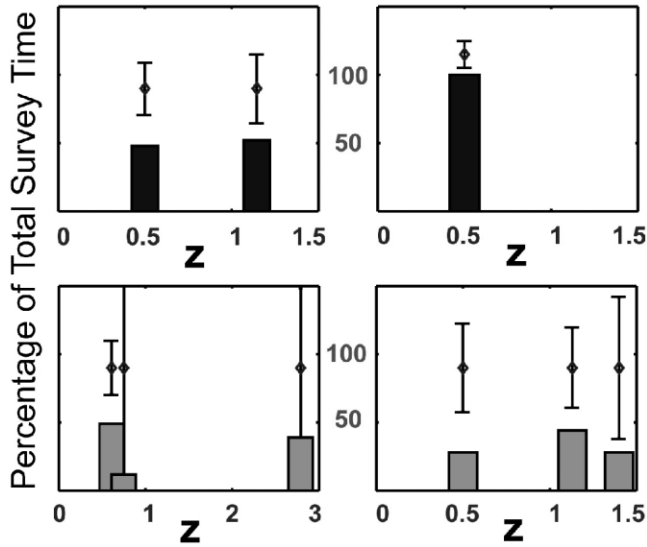


FIG. 4.—Redshifts and integration times for the optimal surveys shown in Fig. 2 and the resulting error bars on $H(z)$. *Top left*: D -optimal maximum FoM (which also has the minimum error ellipse area). It splits the total survey equally between $z = 0.5$ and $z = 1.15$. *Top right*: Thinnest possible ellipse with all measurements at a single redshift, $z = 0.5$. The bottom two panels show the geometries for the second (*left*) and 2000th (*right*) largest figures of merit (only 0.005% and 6% smaller than the maximum, respectively). This shows the diversity of geometries with nearly degenerate figures of merit. [See the electronic edition of the *Journal* for a color version of this figure.]

lows very rapid evolution in $w(z)$, which actually provides a very good fit to current Type Ia supernova data (Bassett et al. 2004). We found that the redshifts of the two bins with the most integration time were typically located at $z < 2$.

5. CONCLUSIONS

We have considered optimization of two-dimensional surveys, such as CMB and weak lensing experiments, and of three-dimensional redshift surveys. In a simplified optimization of a baryon oscillation survey, we have shown how IPSO-allowed significant gains in the statistical power of a survey can be achieved through optimization, in this case a reduction by a factor of 6 in the error ellipse area over the unoptimized survey. We found that there are many diverse surveys with nearly degenerate figures of merit, as shown in Figures 2 and 4. This is good news since it allows survey designers to pick a near-optimal survey structure that is most compatible with real-world intangibles that cannot easily be included explicitly in the optimization.

The MCMC search was repeated thousands of times with randomly chosen initial survey configurations. Most of the resulting locally optimal surveys divided $>90\%$ of the survey time between only two or three redshift bins. A single bin leads to the thinnest possible error ellipse and may be appropriate for some experiments, particularly if the resulting ellipse is orthogonal to those coming from other observations. Alternatively, at almost the same FoM, one can choose a survey configuration that gives the best joint constraints on all the parameters simultaneously. At least for measurements of the Hubble constant alone, we found that typically the two dominant redshift bins should be located at low redshift, $z < 2$, as shown in Figure 4. This is good news for upcoming baryon oscillation surveys such as KAOS that will be able to probe the optical region $z < 1.3$ with high precision from Earth.

We thank Chris Blake, Eric Linder, and Takahiro Tanaka for useful comments on the draft.

REFERENCES

- Amendola, L., Quercellini, C., & Giallongo, E. 2004, preprint (astro-ph/0404599)
- Bassett, B. A. 2004, preprint (astro-ph/0407201) (B04)
- Bassett, B. A., Corasaniti, P. S., & Kunz, M. 2004, *ApJ*, 617, L1
- Blake, C., & Glazebrook, K. 2003, *ApJ*, 594, 665
- Chevallier, M., Polarski, D., & Starobinsky, A. 2001, *Int. J. Mod. Phys. D*, 10, 213
- Christensen, N., & Meyer, R. 2000, preprint (astro-ph/0006401)
- Frieman, J. A., Huterer, D., Linder, E. V., & Turner, M. S. 2003, *Phys. Rev. D*, 67, 083505
- Hu, W., & Tegmark, M. 1999, *ApJ*, 514, L65
- Huterer, D., & Turner, M. S. 2001, *Phys. Rev. D*, 64, 123527
- Jaffe, A. H., Kamionkowski, M., & Wang, L. 2000, *Phys. Rev. D*, 61, 083501
- Kaiser, N. 1992, *ApJ*, 388, 272
- Kesden, M., Cooray, A., & Kamionkowski, M. 2002, *Phys. Rev. Lett.*, 89, 011304
- Knox, L. 1995, *Phys. Rev. D*, 52, 4307
- Knox, L., & Song, Y.-S. 2002, *Phys. Rev. Lett.*, 89, 011303
- Linder, E. V. 2003a, *Phys. Rev. Lett.*, 90, 091301
- . 2003b, *Phys. Rev. D*, 68, 083504
- Rhodes, J., et al. 2004, *Astropart. Phys.*, 20, 377
- Seo, H. J., & Eisenstein, D. J. 2003, *ApJ*, 598, 720
- Tegmark, M., Eisenstein, D. J., Hu, W., & Kron, R. 1998, preprint (astro-ph/9805117)
- Yamamoto, K., Bassett, B. A., & Nishioka, H. 2005, *Phys. Rev. Lett.*, 94, 051301